AMERICAN SOCIETY FOR MICROBIOLOGY | Journal of Virology®

VIRUS-CELL INTERACTIONS

Deletion of the Vaccinia Virus B1 Kinase Reveals Essential Functions of This Enzyme Complemented Partly by the Homologous Cellular Kinase VRK2

Annabel T. Olson,[a,c] Amber B. Rico,[a,b] Zhigang Wang,[a] Gustavo Delhon,[b] Matthew S. Wiebe[a,b]

Nebraska Center for Virology,[a] School of Veterinary Medicine and Biomedical Sciences,[b] and School of Biological Sciences,[c] University of Nebraska, Lincoln, Nebraska, USA

ABSTRACT The vaccinia virus B1 kinase is highly conserved among poxviruses and is essential for the viral life cycle. B1 exhibits a remarkable degree of similarity to vaccinia virus-related kinases (VRKs), a family of cellular kinases, suggesting that the viral enzyme has evolved to mimic VRK activity. Indeed, B1 and VRKs have been demonstrated to target a shared substrate, the DNA binding protein BAF, elucidating a signaling pathway important for both mitosis and the antiviral response. In this study, we further characterize the role of B1 during vaccinia infection to gain novel insights into its regulation and integration with cellular signaling pathways. We begin by describing the construction and characterization of the first B1 deletion virus (vvΔB1) produced using a complementing cell line expressing the viral kinase. Examination of vvΔB1 revealed that B1 is critical for the production of infectious virions in various cell types and is sufficient for BAF phosphorylation. Interestingly, the severity of the defect in DNA replication following the loss of B1 varied between cell types, leading us to posit that cellular VRKs partly complement for the absence of B1 in some cell lines. Using cell lines devoid of either VRK1 or VRK2, we tested this hypothesis and discovered that VRK2 expression facilitates DNA replication and allows later stages of the viral life cycle to proceed in the absence of B1. Finally, we present evidence that the impact of VRK2 on vaccinia virus is largely independent of BAF phosphorylation. These data support a model in which B1 and VRK2 share additional substrates important for the replication of cytoplasmic poxviruses.

IMPORTANCE Viral mimicry of cellular signaling modulators provides clear evidence that the pathogen targets an important host pathway during infection. Poxviruses employ numerous viral homologs of cellular proteins, the study of which have yielded insights into signaling pathways used by both virus and cells alike. The vaccinia virus B1 protein is a homolog of cellular vaccinia virus-related kinases (VRKs) and is needed for viral DNA replication and likely other stages of the viral life cycle. However, much remains to be learned about how B1 and VRKs overlap functionally. This study utilizes new tools, including a B1 deletion virus and VRK knockout cells, to further characterize the functional links between the viral and cellular enzymes. As a result, we have discovered that B1 and VRK2 target a common set of substrates vital to productive infection of this large cytoplasmic DNA virus.

KEYWORDS B1R, BAF, BANF1, VRK2, poxviruses, protein kinases, vaccinia

Received 13 April 2017 **Accepted** 10 May 2017

Accepted manuscript posted online 17 May 2017

Citation Olson AT, Rico AB, Wang Z, Delhon G, Wiebe MS. 2017. Deletion of the vaccinia virus B1 kinase reveals essential functions of this enzyme complemented partly by the homologous cellular kinase VRK2. J Virol 91:e00635-17. https://doi.org/10.1128/JVI.00635-17.

Editor Grant McFadden, The Biodesign Institute, Arizona State University

Address correspondence to Matthew S. Wiebe, mwiebe@unl.edu.

Poxviruses are large double-stranded DNA (dsDNA) viruses, which carry out all stages of their life cycle in the cytoplasm of infected cells (1). Vaccinia virus, the prototypical poxvirus, has a genome 195 kb in size that encodes approximately 200 proteins (2). These proteins are expressed in a temporally regulated cascade of early, interme-

diate, and late stages of gene expression. Close to half of poxviral proteins are expressed early in infection and include virally encoded DNA replication machinery and viral transcription factors (2). Also among the early proteins are numerous viral factors capable of interacting with host proteins and modulating host signaling cascades (3). Studies of the host mechanisms targeted by vaccinia virus proteins have provided fascinating insights into how cellular signaling can be redirected to create an environment favorable to an infecting pathogen.

The vaccinia virus B1 protein kinase is essential for productive infection and has a clear role in impairing at least one facet of the host antiviral response. B1 homologs are highly conserved within the members of the *Poxviridae* family that infect mammals, with the only exceptions being the *Molluscipoxvirus* and *Parapoxvirus* genera. Much of what we know regarding the function of B1 is based on studies of temperature-sensitive mutant viruses (Cts2 and Cts25) with point mutations in the B1 locus (4, 5, 46). Biochemical and genetic analyses of these mutant viruses and kinases indicate that during infection, the altered proteins are expressed but are considerably more labile than wild-type B1 and have severely reduced catalytic activity (6). Phenotypically, progeny of these B1-deficient viruses are markedly reduced in number during infection at nonpermissive temperatures, due to critical defects in viral DNA replication (4, 6). Importantly, while wild-type B1 is vital to productive infection in all cell lines tested to date, the severity of the Cts2 virus phenotype is cell type dependent (5, 7, 8). This suggests that functional activity of the mutant B1 protein and/or its substrates may be impacted by host enzymes, which may partially complement for B1 in some cell types. The discovery that a group of eukaryotic serine/threonine kinases have homology (~40% identity) to the vaccinia virus *B1* gene led them to be named vaccinia virus-related kinases (VRKs) (9–11). Importantly, this discovery supports the model that B1 activity may be complemented in some cells by these host enzymes. Indeed, functional conservation of these viral and cellular kinases has been demonstrated by (i) evidence that VRK1 can rescue the Cts2 viral DNA replication defect when expressed from the Cts2 virus genome under a viral promoter (12), and (ii) the discovery that B1 and VRK1 share the same cellular substrate (13), the barrier to autointegration factor (BAF) encoded by the *BANF1* gene. Mammals express three VRK proteins which exhibit clear homology within their respective kinase domains (11). However, other regions of the proteins are unique and are responsible for directing the VRKs to distinct subcellular localizations. For example, VRK1 is located predominantly in the nucleus, while the major isoform of VRK2 is associated with the endoplasmic reticulum (ER) and nuclear envelope (11, 14). Interestingly, both VRK1 and VRK2 possess strong catalytic activity found to modulate cellular processes, including mitosis and apoptosis, via multiple substrates (15–18). It has also been demonstrated that VRK2 limits cell death during Epstein-Barr virus (EBV) infection (19) and delays myxoma virus replication in a breast cancer cell line (20), thus providing other examples that VRKs may regulate pathways important during viral infection.

The most well characterized substrate of both B1 and the VRKs is BAF, a highly conserved DNA-binding protein with essential cellular functions. BAF expression is needed for survival and differentiation of both human and mouse embryonic stem cells, and the depletion or knockout of BAF in *Caenorhabditis elegans* and *Drosophila melanogaster* is embryonically lethal to those animals (21, 22). BAF has also been implicated in human disease; a point mutation within the BAF coding region has been identified in two patients presenting with a hereditary progeroid disease called Nestor-Guillermo progeria syndrome (23). The molecular underpinnings of these defects are likely multifactorial (24), as BAF functions during mitosis and other processes integral to maintaining genomic integrity (45). In addition to these cellular functions, BAF is also capable of strongly inhibiting vaccinia virus DNA replication (25, 26) and intermediate transcription (27). The host defense activity of BAF against vaccinia virus is dependent on its DNA-binding property, which can be blocked through phosphorylation mediated by B1 (25, 28), thus highlighting the importance of this kinase during poxvirus DNA replication.

Despite the fact that the vaccinia virus B1 kinase and the cellular VRK proteins share similar kinase domains and can all target BAF, it remains to be determined whether the VRK proteins expressed by the cell can regulate BAF antiviral activity or if B1 and the VRKs may share other substrates important for poxviral infection. The purpose of this study was to address these and other knowledge gaps in B1/VRK signal transduction. Here, we describe the construction and characterization of the first recombinant vaccinia virus in which the entire B1 coding sequence has been deleted. This was achieved using a complementing cell line expressing the B1 protein and allowed us to thoroughly examine the role of B1 independent of any residual hypomorphic activity present for the B1 temperature-sensitive mutant proteins. Next, we determined that B1-mediated phosphorylation of BAF is not enhanced by other viral factors nor does BAF hyperphosphorylation occur during infection in the absence of B1. Furthermore, using the B1 deletion virus, we present evidence that VRK2 and, to a lesser degree, VRK1 can complement for the absence of B1. Intriguingly, the complementation of the B1 deletion virus by VRK2 appears to occur via a mechanism that is largely independent of BAF, thus indicating that B1 and VRK2 share a novel signaling pathway capable of significantly regulating the poxvirus life cycle.

RESULTS

Construction of a B1-complementing cell line and B1 deletion vaccinia virus. To gain further insight into the functions of the vaccinia virus B1 kinase, we initiated construction of a mutant virus in which the B1R open reading frame (ORF) is deleted. In light of the previous observation that B1 expression is essential to the viral life cycle (12), we posited that replication of a *B1R* deletion virus would require a complementing cell line expressing the kinase. Therefore, a lentivirus system was used to stably express a myc-tagged B1 kinase (B1myc) codon optimized for expression in mammalian cells. Transduced CV1 cells were confirmed to have B1myc expression by immunoblot analysis (Fig. 1A). To determine whether stable expression of B1 resulted in any gross changes in cell fitness, the morphology of the cells was closely monitored, as was their doubling rate over time. We observed no alteration in the morphology of B1myc-expressing cells over a period of 3 to 4 weeks (data not shown). Furthermore, CV1 cells expressing the B1myc protein (CV1-B1myc cells) did not differ significantly from the control cells in regard to apparent doubling time (Fig. 1B). Finally, we used an immunofluorescence assay to determine the localization of the B1myc protein in transduced cells. We observed that the B1myc protein was present primarily in the cytoplasmic compartment in uninfected cells (Fig. 1C). Together, these data illustrate that we successfully produced a cell line stably expressing the B1myc protein in the cytoplasmic compartment.

To next construct a B1 deletion virus (vvΔB1), we utilized a targeting construct in which the mCherry ORF was placed downstream of the vaccinia P11 late promoter and flanked by ~250 bp homologous to the sequence immediately upstream and downstream of the B1R ORF in the vaccinia virus strain WR genome (Fig. 2A). This targeting construct containing the mCherry ORF was transfected into CV1-B1myc cells infected with wild-type (WT) vaccinia virus, and recombinant progeny were identified using fluorescence microscopy. Virus expressing mCherry was purified by serial plaque purification on CV1-B1myc cells until no nonfluorescent plaques (out of 100 plaques) were observed and then plaque purified an additional six times. This virus was then expanded on CV1-B1myc cells, and replacement of the B1R ORF was verified by PCR using primer sets 1 to 3 (Fig. 2A) and DNA sequencing (data not shown). Upon confirmation of the sequence of the newly purified recombinant virus, we began characterization of the B1 deletion virus by immunofluorescence assays and comparative growth studies with the temperature-sensitive Cts2 virus detailed below. Microscopy studies using WT and vvΔB1 viruses in control CV1 cells and B1myc-expressing cells revealed that replication factories are similar in size and number for WT and vvΔB1 viruses in B1-complementing cell lines but absent for vvΔB1-infected control cells (Fig. 2B, αI3 panel, white arrowheads). Additionally, B1myc localizes to I3 during both WT

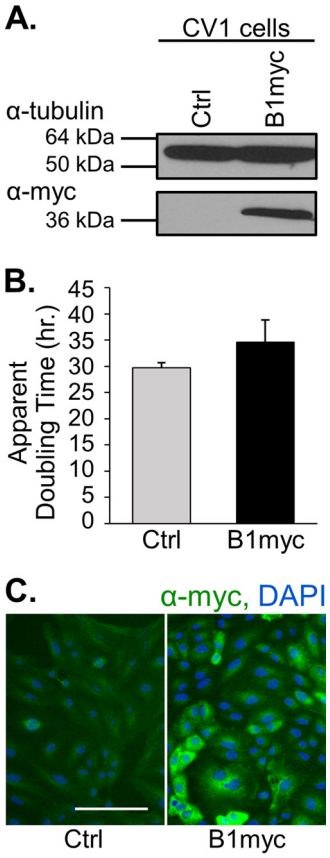

FIG 1 Characterization of CV1 cells stably expressing myc-tagged B1 kinase. (A) Representative immunoblot analysis of CV1 whole-cell lysates of control cells or B1myc-expressing cells using anti-myc or anti-tubulin primary antibodies. (B) The apparent doubling times of CV1 control ($n = 2$) and B1myc-expressing ($n = 5$) cells were calculated. Error bars represent standard deviations. (C) Immunofluorescence analysis of B1myc protein localization in uninfected CV1 control and B1myc transduced cells. The B1myc protein was detected using anti-myc primary antibody with the appropriate secondary antibody, and DAPI was used to detect the cellular nucleus.

and vvΔB1 infection (Fig. 2B, white arrowheads), although it is dispersed in the cytoplasm in the absence of infection (Fig. 1C). Based on these initial results, vvΔB1 behaves similarly to the WT virus in CV1-B1myc cells in relation to the presence of replication foci and B1 recruitment to replication foci.

B1 expression in CV1 cells rescues viral growth of both Cts2 and vvΔB1 to nearly WT levels. Next, we characterized vvΔB1 using a plaque assay and a one-step viral yield assay in CV1 control cells and CV1-B1myc cells. For comparison, the well-characterized temperature-sensitive virus Cts2 was also included in these assays. Importantly, the Cts2 virus is able to complete the viral life cycle and produce infectious virions at low temperature (31.5°C) but is inhibited at the stage of DNA replication at high temperature (39.7°C) (5, 6). In the Cts2 virus, the *B1R* gene contains a single nucleotide substitution that results in the expression of a more labile and catalytically inert protein (6). Therefore, we predicted that the CV1-B1myc cells will complement the Cts2 virus as well as our new recombinant virus, vvΔB1. Indeed, B1myc expression rescued the Cts2 virus at a nonpermissive temperature (39.7°C) and the vvΔB1 virus at a low multiplicity of infection (MOI) as assayed using a plaque assay (Fig. 2C). Specifically, the number of plaques for Cts2 and vvΔB1 viruses increased from 0 to about 200 plaques, although it is noteworthy that the plaque morphology of both Cts2 and vvΔB1 resulted in slightly smaller plaques than those produced by the WT virus. Additionally, the WT virus plaque numbers and morphology were not altered by the expression of B1myc in CV1 cells, demonstrating that B1 expression from the cell does not enhance WT viral growth at a low MOI.

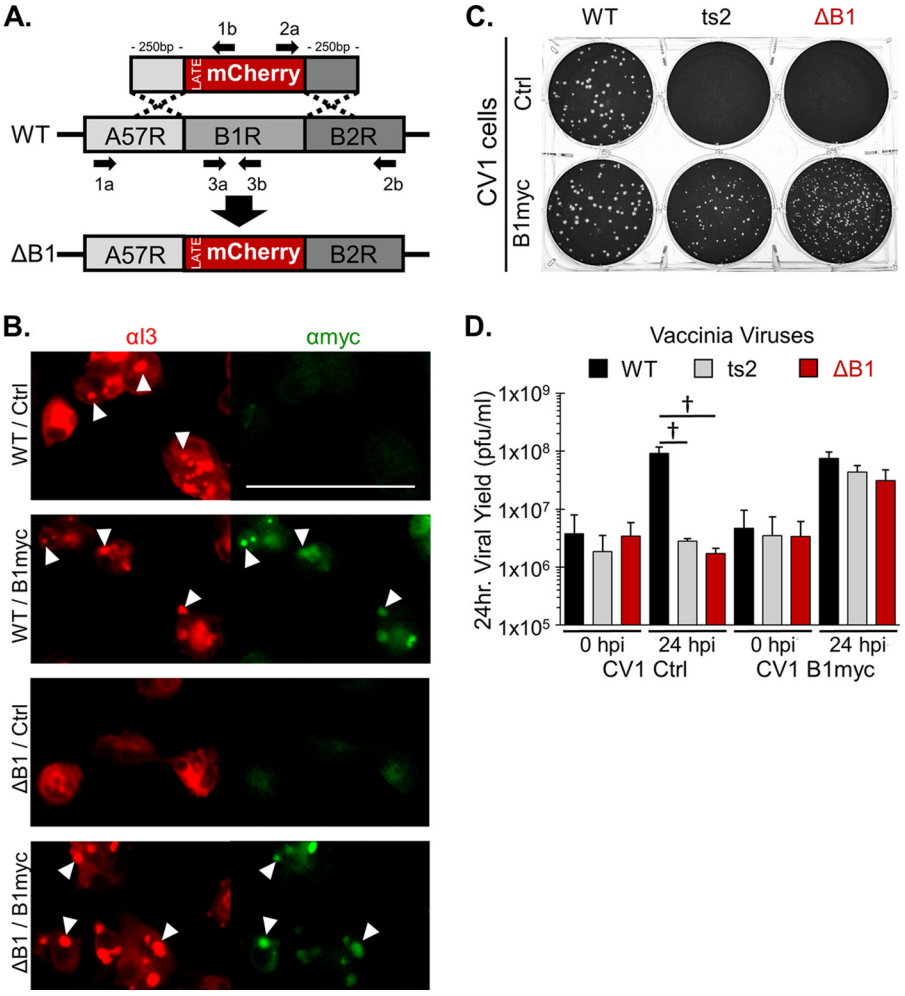

FIG 2 Knockout strategy and growth characteristics of vvΔB1 in CV1 cells. (A) The B1 deletion virus was generated via homologous recombination between the WT WR vaccinia virus genome and a DNA fragment of the mCherry gene with a 250-bp homologous sequence to the regions flanking the B1 gene, replacing the B1 gene with the mCherry gene under a late viral promoter, P11. Arrows indicate primer sets used to amplify DNA used for sequence confirmation of recombination. (B) Immunofluorescence analyses of CV1 control and B1myc cells infected with WT or vvΔB1 virus at an MOI of 5 for 7 h at 37°C before fixation. Detection of I3 (red) used anti-I3 primary antibody, and B1myc (green) detection used anti-myc primary antibody. White arrowheads point to I3 (red) foci representative of DNA replication factories (left panels) and B1myc (green) foci colocalizing with I3 (right panels, B1myc cells only). The late mCherry fluorescent protein produced during vvΔB1 infection was not above background levels at 7 hpi (data not shown). (C) Plaque assay of control (top row) and B1myc-expressing (bottom row) CV1 cells infected with 200 PFU per well of WT, Cts2, or vvΔB1 virus. Cells were incubated for 72 h at 39.7°C prior to fixation and staining. (D) Twenty-four-hour viral yield assays were carried out at 39.7°C for WT (black), Cts2 (gray), and vvΔB1 (red) viruses on control (left three bars) and B1myc-expressing (right three bars) CV1 cells. Virus titrations were completed on B1myc-expressing cells at 31.5°C. Standard deviation is denoted by error bars, and a dagger indicates a *P* value of <0.05.

Production of infectious virus during Cts2 and vvΔB1 infection was then assessed through a one-step 24-h infection and titration of virus. In the CV1 control cells (at 39.7°C), both the Cts2 and vvΔB1 viral yields were reduced about 32- and 53-fold, respectively, compared to the WT viral yield (Fig. 2D). We found that this decrease in yield could be rescued for Cts2, but not for the vvΔB1 virus (data not shown), if the assay was done at 31.5°C, thus demonstrating that vvΔB1 is not temperature sensitive. Next, the same assays were performed in CV1-B1myc cells. Expression of B1 in these cells did not significantly alter WT viral yield from levels in control cells. However, infections of the CV1-B1myc cells revealed a significant rescue of both the Cts2 and vvΔB1 to nearly WT levels for viral yield. Specifically, B1myc expression from the cells increased Cts2 and vvΔB1 viral yields 16- and 18-fold, respectively, over the viral yield

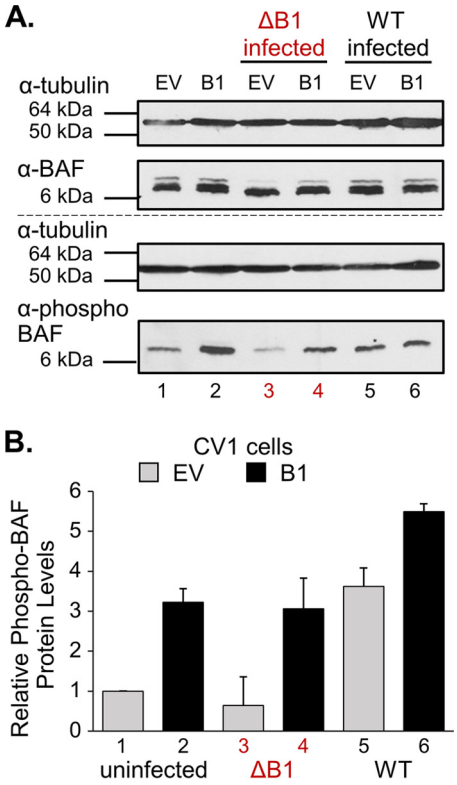

FIG 3 B1 is necessary and sufficient to phosphorylate BAF in cultured cells. (A) Whole-cell lysates were harvested from CV1 control (EV) or B1myc-expressing (B1) cell lines which were uninfected (lanes 1 and 2) or infected with vvΔB1 (lanes 3 and 4, red) or WT (lanes 5 and 6) virus at an MOI of 10 for 6 h at 37°C. The top panel is a representative immunoblot assayed for the tubulin loading control and total BAF protein levels. The same lysates were used to generate the bottom panel of the tubulin loading control and phosphorylated BAF form as detected by the phosphospecific BAF antibody. (B) Relative phospho-BAF/total BAF protein levels were quantified using ImageLab software (Bio-Rad), and error bars represent standard deviations ($n = 4$). The value for the uninfected EV sample was set to 1. The numbers under each column correspond to the numbering for the immunoblot in panel A.

in control cells (Fig. 2D). Together, these data provide evidence that deletion of B1 from the viral genome results in a severe, temperature-independent loss in viral fitness and that B1 expression from the cell can complement for this defect.

B1 expression in CV1 cells is necessary and sufficient to hyperphosphorylate BAF independent of other viral factors. Previous studies of the B1 kinase determined that this kinase is needed to directly regulate the phosphorylation and thus the antiviral activity of BAF, a cellular DNA binding protein. Specifically, hyperphosphorylated BAF has reduced affinity for dsDNA and reduced homodimerization activity, both of which are required to facilitate dsDNA condensation and inhibition of vaccinia virus DNA replication and intermediate transcription (13, 27–29). Despite our growing understanding of this B1-BAF signaling axis, it is unknown if the B1 kinase activity mediating BAF phosphorylation in cells is enhanced by other viral factors. To address this gap in knowledge, we utilized both the B1myc-expressing CV1 cells and vvΔB1 to determine if B1myc expression in cells in the absence of infection results in BAF phosphorylation to levels similar to that produced by WT infection. First, lysates from uninfected control cells or CV1-B1myc cells were used for an immunoblot analysis of total BAF protein levels and phosphospecific BAF protein levels. Total BAF protein levels were similar between the CV1 control cells (Fig. 3A, lane 1, top panel) and the CV1-B1myc-transduced cells (lane 2, top panel), whereas phosphospecific BAF protein levels were markedly higher in cells stably expressing the B1myc protein than in empty vector (EV)-transduced cells (Fig. 3A, compare lanes 1 and 2 in bottom panel). Quantitation of the relative phosphorylated BAF (phospho-BAF) protein levels from four independent

experiments are graphed and demonstrate that, on average, >3-fold more phosphorylated BAF is found in B1myc-expressing cells than in control cells (Fig. 3B). These data support the conclusion that B1myc alone is able to upregulate BAF phosphorylation independent of other viral factors.

We next addressed the question of whether another viral factor(s) enhances B1-mediated BAF phosphorylation. CV1 control cells and B1myc-expressing cells were infected with either WT virus or vvΔB1. Cell lysates isolated at 6 h postinfection (hpi) were used for analysis of total BAF and phospho-BAF levels. In regard to total BAF protein, we observed similar levels for uninfected and infected cell lysates of both EV (empty vector) control and B1myc-expressing CV1 cells (Fig. 3A, top panel). In regard to phosphorylated BAF, vvΔB1-infected control CV1 cells consistently showed phospho-BAF levels similar to those in uninfected control CV1 cells (Fig. 3A, compare lanes 1 and 3 in lower panel). In comparison, B1myc expression from cells during vvΔB1 infection rescues phospho-BAF levels by approximately 3-fold, which is similar to the fold increase between uninfected CV1-B1myc cells and WT-infected control cells (Fig. 3B, compare column 4 to columns 1 and 5). Another observation was that WT-infected CV1-B1myc cells had, on average, higher phospho-BAF levels, but no significant change in plaque formation or viral yield was observed (Fig. 2B and C). Overall, the finding of no difference between BAF phosphorylation levels in Fig. 3B (columns 2 and 4) argues against another vaccinia virus protein enhancing B1 phosphorylation of BAF. Together, these data support previous evidence that B1 kinase is necessary to phosphorylate BAF in cells. Furthermore, our data provide new evidence that this mechanism occurs independently of other viral factors, as phosphorylation of BAF is not enhanced in the presence of other viral proteins.

BAF depletion results in a partial rescue of vvΔB1 replication. BAF depletion strongly rescues both viral DNA replication and viral yield during Cts2 infection (25), demonstrating that a primary function of B1 is to inactivate the antiviral activity of BAF. Based on those data, we hypothesized that depletion of BAF would similarly rescue the growth of vvΔB1. To test this prediction, lentiviral expression of BAF-specific short hairpin RNA (shRNA) was used to deplete endogenous BAF to about 20% of the total BAF protein in CV1 cells (Fig. 4A). A plaque assay was used to assess viral growth at a low MOI in control cells and BAF-depleted cells. WT virus maintained plaque size and number independent of BAF depletion, as expected. The Cts2 virus plaque number was rescued by BAF depletion at a nonpermissive temperature, which is consistent with previous studies utilizing this model. However, as seen before, the Cts2 plaque size is noticeably smaller than that of the WT (12). Therefore, both B1myc-expressing cells (Fig. 2C) and BAF-depleted cells (Fig. 4B) rescue Cts2 deficiency in plaque number. vvΔB1, however, was not rescued by BAF depletion at a low MOI infection; no visible plaques were present in either the control or the BAF-depleted CV1 cells (Fig. 4B). These results indicate that CV1-B1myc cells (Fig. 2C) but not BAF-depleted cells (Fig. 4B) rescue the vvΔB1 plaque numbers to WT levels at a low MOI.

Subsequent studies were conducted at a higher MOI to determine DNA replication and viral yield of the vvΔB1 virus in the BAF-depleted cells. WT DNA replication remained constant independently of BAF depletion, representing control conditions with a functional B1 kinase produced by vaccinia virus (Fig. 4C, columns 1 and 4). During Cts2 and vvΔB1 infections of short hairpin control (shCtrl) CV1 cells, 75% and 96% reductions in DNA accumulation, respectively, were observed in comparison to that from WT infection of shCtrl cells (Fig. 4C). In comparison, DNA accumulation during Cts2 infection of BAF-depleted CV1 cells was reduced only about 13% from that during WT infection, while DNA replication of vvΔB1 remained 72% attenuated in BAF-depleted cells (Fig. 4C). Therefore, BAF depletion rescued Cts2 DNA accumulation to near WT levels, but vvΔB1 still exhibited attenuation in cells depleted of BAF. To next examine the impact of BAF depletion on the production of infectious virus, one-step viral yield assays were undertaken. We observed that the Cts2 and vvΔB1 viral yields were reduced 71- and 170-fold in comparison to WT viral yields during infection of CV1

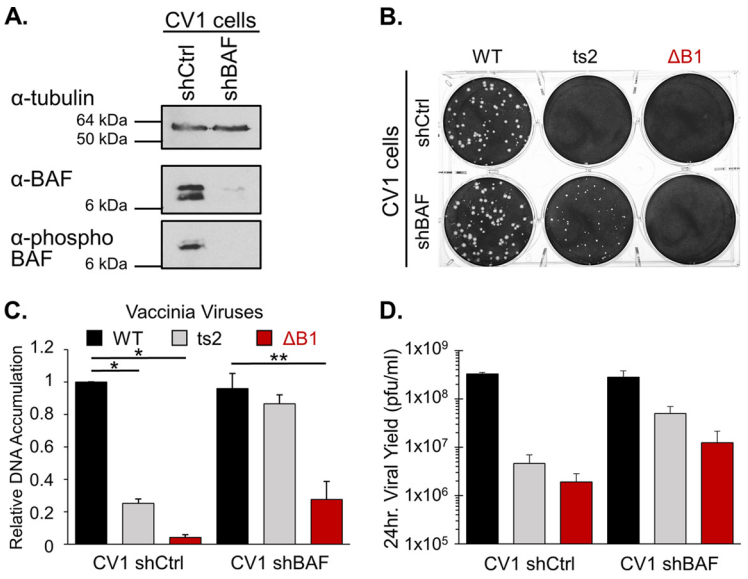

FIG 4 Impact of BAF depletion on growth of B1 mutant viruses. (A) Representative immunoblot analysis of BAF in CV1 cells transduced to express shCtrl or shBAF. Detection of tubulin (top panel) was used as a loading control. Total BAF (middle panel) and phospho-BAF (bottom panel) levels were detected using anti-BAF and anti-phospho-BAF primary antibodies, respectively. (B) Plaque assay on control (top row) and BAF-depleted (bottom row) CV1 cells infected with 200 PFU of WT, Cts2, or vvΔB1 virus per well. Cells were incubated for 72 h at 39.7°C prior to fixation and imaging. (C and D) One-step DNA accumulation (C) and viral yield (D) assays were completed at 39.7°C for WT, Cts2, and vvΔB1 virus on shCtrl and shBAF CV1 cells. The value for the WT/CV1 shCtrl sample was set to 1 for relative DNA accumulation. Virus titers were quantified on B1myc-expressing cells at 31.5°C (permissive temperature for Cts2 virus). Standard deviation is denoted by error bars, and *P* values are indicated as follows: *, <0.005; **, <0.001 (horizontal black lines indicate compared columns).

cells expressing a control shRNA (Fig. 4D). However, the Cts2 and vvΔB1 virus yields were about 6- and 23-fold lower than the WT virus yield, respectively, in the BAF-depleted cell infections (Fig. 4D). Therefore, BAF depletion cannot fully rescue vvΔB1 DNA replication and viral yield to WT levels. These results revealed an enhanced deficiency of vvΔB1 DNA replication and viral yield in comparison to the Cts2 virus. It appears that while the B1 mutant protein expressed by Cts2 is highly labile and catalytically inert at high and low temperatures (6), it still makes a substantial contribution to the viral life cycle either by regulating BAF or possibly by participating in additional, unknown signaling pathways.

The vvΔB1 virus displays a growth-deficient phenotype in multiple cell lines. We next examined whether vvΔB1 exhibited cell type-specific variability in its replication. Previous work using Cts2 and Cts25, another temperature-sensitive B1 mutant virus, showed reduced viral growth in mouse L929 cells compared to that in BSC40 cells at a nonpermissive temperature (5, 6), suggesting that the mutant B1 virus and/or its substrates may function in a cell type-specific manner. If it is the substrates rather than the mutant B1 virus that is cell type dependent, then one would predict that vvΔB1 would have a similar trend as the Cts2 virus, attenuated viral growth overall, and increased deficiency in the mouse L929 cell line. Interestingly, our results showed that DNA replication was attenuated for the vvΔB1 virus to similar degrees in monkey, mouse, and human cell lines, with no increased deficiency in the L929 mouse cells as was previously found with Cts2 (6) (Fig. 5A and C). Virus production was also profoundly diminished, with the vvΔB1 viral yields being 448-, 176-, and 668-fold lower than the WT viral yield in the BSC40, CV1, and L929 cell lines, respectively (Fig. 5B), and 650-fold lower than the WT viral yield in HeLa cells (Fig. 5D). Together, these data demonstrate that the loss of B1 results in a significant decrease in viral fitness that can be observed in diverse cell types.

VRK2 is required in HAP1 cells for optimal DNA replication of vvΔB1. The vaccinia virus B1 kinase has ~40% sequence identity to a family of conserved cellular

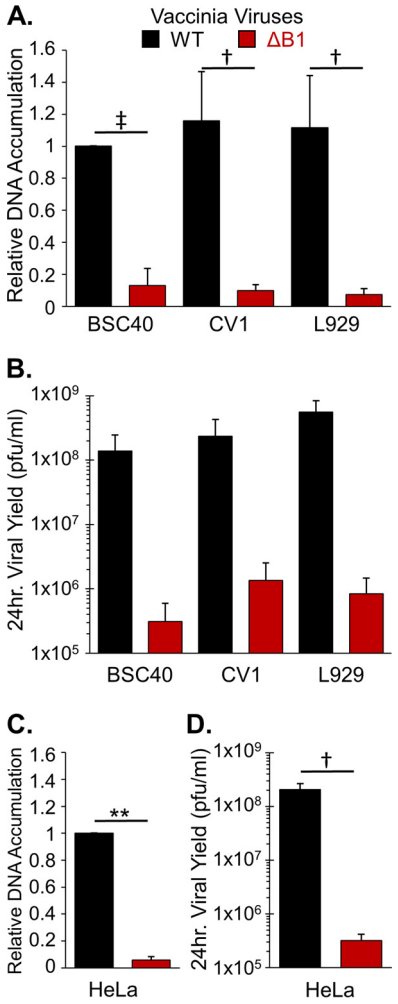

FIG 5 Growth of vvΔB1 in multiple cell types. One-step infections were done at an MOI of 3 for WT (black) or vvΔB1 (red) virus on BSC40, CV1, L929, or HeLa cells incubated at 37°C. Cells and virus were harvested at 24 hpi. (A) DNA accumulation for BSC40, CV1, and L929 cells. The value for the WT/BSC40 sample was set to 1. (B) Viral yield for infections in BSC40, CV1, and L929 cells. Virus titrations were completed on B1myc-expressing CV1 cells. (C and D) HeLa cell DNA accumulation (C) and viral yield (D) assays were conducted separately from those for other cell lines, using an identical protocol. The value for the WT/HeLa sample was set to 1. Titers of viral harvest were determined on CV1-B1myc cells. Standard deviation is denoted by error bars, and *P* values are indicated as follows: †, <0.05; ‡, <0.01; **, <0.001 (horizontal black lines indicate compared columns).

genes called vaccinia virus-related kinases (VRKs) from which it likely evolved (9). VRKs have essential roles within cells, one of which is to mediate BAF regulation during mitosis. *In vivo* VRK1 regulates BAF function in the nucleus via phosphorylation (16), and *in vitro* studies determined that both VRK1 and VRK2 are able to phosphorylate BAF (13). Complementation studies for B1 kinase were completed previously, using VRK1 recombined into the Cts2 virus. In those studies, VRK1 expressed under a viral promoter in the cytoplasmic compartment rescued viral DNA replication deficiency of the Cts2 virus to greater than WT levels, although plaque morphology was smaller for Cts2-VRK1 recombinant virus than for the WT control (12). These studies confirmed complementation under conditions which circumvent the nuclear restriction of endogenous VRK1. Therefore, we hypothesized that endogenous VRKs would compensate for the absence of the viral B1 kinase during infection. To test this hypothesis, we used a human, nearly haploid (HAP1) cell line control and VRK1 or VRK2 knockout (KO) HAP1 cell lines to evaluate the requirement of VRK1 or VRK2 during infection with the vvΔB1 virus. First, we confirmed the loss of expression of either VRK1 or VRK2 from the knockout HAP1

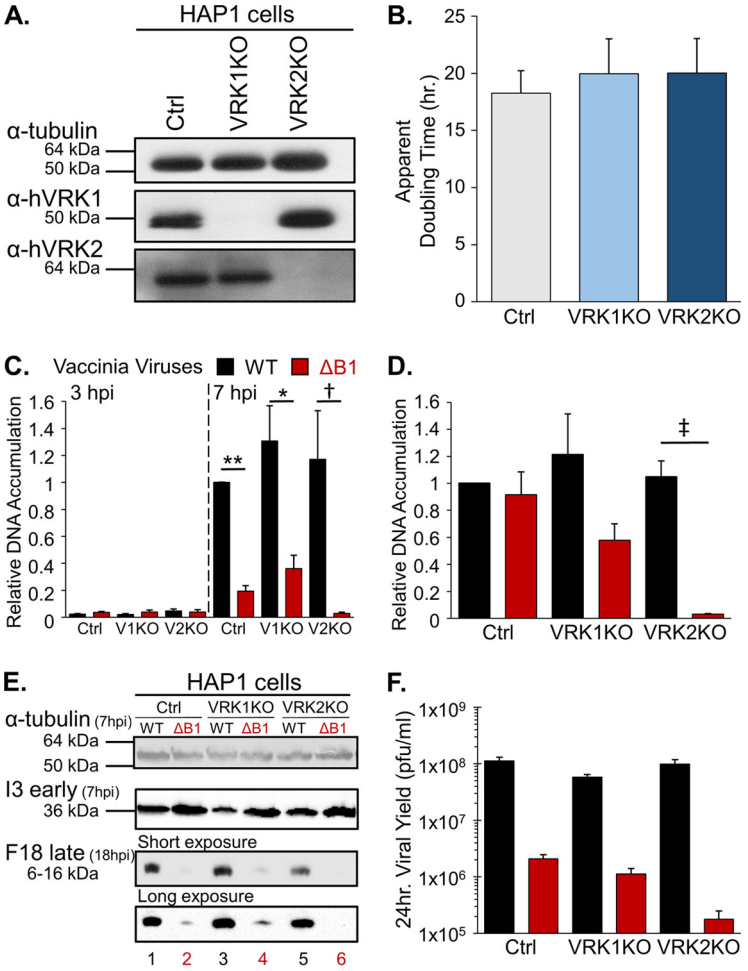

FIG 6 VRK2 and to a lesser extent VRK1 complement B1 roles in DNA replication and viral yield production of vvΔB1. (A) HAP1 cell lysates from control, VRK1KO, and VRK2KO cells were subjected to immunoblot analysis using anti-tubulin, anti-VRK1, or anti-VRK2 primary antibody. (B) The apparent doubling time was calculated for each HAP1 cell line. Standard deviation is denoted by error bars (n = 5). (C) DNA accumulation for 3 hpi (left of dotted line) and 7 hpi (right of dotted line) for WT (black) or vvΔB1 (red) virus in HAP1 control, VRK1KO, or VRK2KO cells. The value for the 3-hpi WT/Ctrl sample was set to 1. (D and F) DNA accumulation (D) and viral yield (F) measured for WT (black) or vvΔB1 (red) virus at 24 hpi in HAP1 cell lines: control, VRK1KO, or VRK2KO cells. The value for the WT/Ctrl sample was set to 1 for DNA accumulation. Standard deviation is denoted by error bars, and P values are indicated as follows: †, <0.05; ‡, <0.01; *, <0.005; **, <0.001. (E) Whole-cell lysates from control (lanes 1 and 2), VRK1KO (lanes 3 and 4), and VRK2KO (lanes 5 and 6) were infected with either WT (lanes 1, 3, and 5) or vvΔB1 (lanes 2, 4, and 6) virus and harvested for immunoblot analysis for both early gene expression (anti-I3) at 7 hpi and late gene expression (anti-F18) at 18 hpi. The cell loading control, tubulin, was detected from 7-hpi cell lysates. The F18-specific blot is shown at both short (top) and long (bottom) exposure times.

cell lines by immunoblot analysis (Fig. 6A). Second, although VRKs are known to regulate the cell cycle (30–34), we observed no significant variability in apparent doubling time between the control and knockout HAP1 cell lines (Fig. 6B). Third, we examined viral DNA accumulation to determine VRK1 or VRK2 complementation of B1 function. WT and vvΔB1 viruses have similar levels of relative DNA present at 3 hpi in HAP1 control, VRK1KO, and VRK2KO cell lines indicative of viral entry but minimal if any DNA replication at this time point (Fig. 6C, left). At 7 hpi, DNA accumulation increased for both viruses but showed a consistent lag during vvΔB1 infection in comparison to WT virus infection in HAP1 control, VRK1KO, and VRK2KO cells (Fig. 6C, right), demonstrating the importance of B1 for DNA replication in these cells. Interestingly, by 24 hpi, the amount of vvΔB1 DNA detected was similar to that of WT virus DNA in the HAP1 control cells, indicating that although vvΔB1 lags at 7 hpi, it can recover if given enough

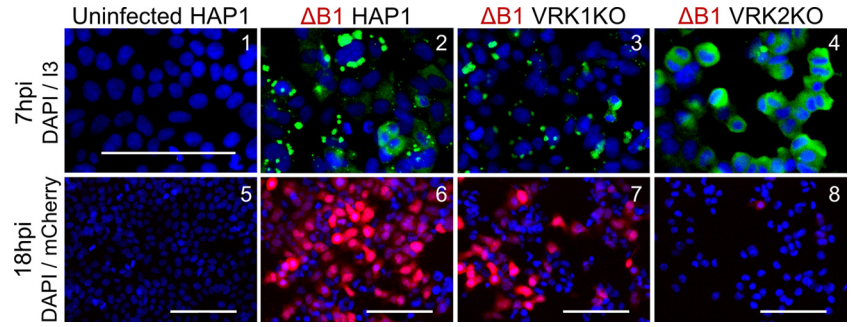

FIG 7 Characterization of vvΔB1 DNA replication factory formation and late mCherry protein levels in HAP1 control, VRK1KO, and VRK2KO cell lines. Immunofluorescence analyses of uninfected HAP1 control cells (panels 1 and 5) and vvΔB1-infected HAP1 control (panels 2 and 6), VRK1KO (panels 3 and 7), and VRK2KO (panels 4 and 8) cells were done at an MOI of 5, with incubation at 37°C. Early I3 protein was detected using anti-I3 primary antibody at 7 hpi (panels 2 to 4), and late mCherry fluorescent protein was imaged from cells at 18 hpi (panels 6 to 8). Uninfected HAP1 control cells were also incubated with anti-I3 primary antibody and appropriate secondary antibody. All cells were incubated with DAPI stain, used to detect nuclei.

time (Fig. 6D). However, vvΔB1 DNA was not as abundant in the VRK1KO or VRK2KO HAP1 cell lines at 24 hpi. Infected VRK1KO cells exhibited a 52% reduction in relative DNA accumulated for vvΔB1 in comparison to that for the WT virus (Fig. 6D). A striking difference was observed in the VRK2KO cells, which showed a further reduction in DNA accumulation during vvΔB1 infection, reaching levels of only 3% DNA accumulation in comparison to the WT total levels. Next, we analyzed the expression of a representative early and late gene to determine if the loss of B1 affected these stages of the virus life cycle in HAP1 cells. Early gene expression, as assayed by the I3 protein level at 7 hpi via immunoblot analysis, was present at similar to slightly higher levels for vvΔB1 than for the WT in HAP1 control, VRK1KO, and VRK2KO cell lines (Fig. 6E). This early gene expression is consistent with unaltered early transcription despite the loss of B1. Late gene expression, as measured by detection of late protein F18 at 18 hpi (Fig. 6E), was markedly reduced during vvΔB1 infection in comparison to that during WT infection in HAP1 control and VRK1KO cells lines, although a low level of expression could be detected in these two cell lines. Importantly, no visible F18 late protein was observed for vvΔB1 in the VRK2KO HAP1 cells. These data are consistent with a model in which the replication of vvΔB1 DNA in control and VRK1 KO cells allows for weak late gene expression, whereas the severely impaired DNA replication in VRK2 KO cells results in a complete block of late gene expression. Finally, we tested the effects of the absence of VRK1 and VRK2 on viral yield for the vvΔB1 virus. Consistent with the late gene expression data, the viral yield was almost 53-fold less for vvΔB1 than for the WT virus in the HAP1 control cells (Fig. 6F). The vvΔB1 viral yield during infection of VRK1KO cells exhibited a 52-fold reduction relative to that during WT infections, similar to the trend observed in HAP1 control cells (Fig. 6F). As observed for the viral DNA replication data (Fig. 6D), an additional reduction in viral fitness occurred in the VRK2KO cells. The viral yield of the vvΔB1 virus in the VRK2KO cells was 550-fold lower than the WT viral yield under the same cellular conditions (Fig. 6F). Lastly, we used an immunofluorescence assay to assess early (I3) and late (P11mCherry) protein expression for vvΔB1 in each HAP1 cell line. The uninfected cells represent the negative controls for I3 and mCherry viral protein expression (Fig. 7, panels 1 and 5). At 7 hpi, the I3 early protein is expressed in vvΔB1-infected parental HAP1 cells and forms foci indicative of replication factories (Fig. 7, panel 2), which is consistent with both I3 protein levels at 7 hpi (Fig. 6E) and DNA accumulation results (Fig. 6C). Interestingly, while I3 was expressed in VRK1KO and VRK2KO cells, the number of concentrated foci formed by I3 decreases in the VRK1KO cell line and these foci are quite rare in VRK2KO cells in comparison to vvΔB1-infected HAP1 control cells (Fig. 7, panels 3 and 4).

Next, late protein expression was assayed through detection of the mCherry protein, in which gene expression is regulated by the P11 late viral promoter. mCherry protein

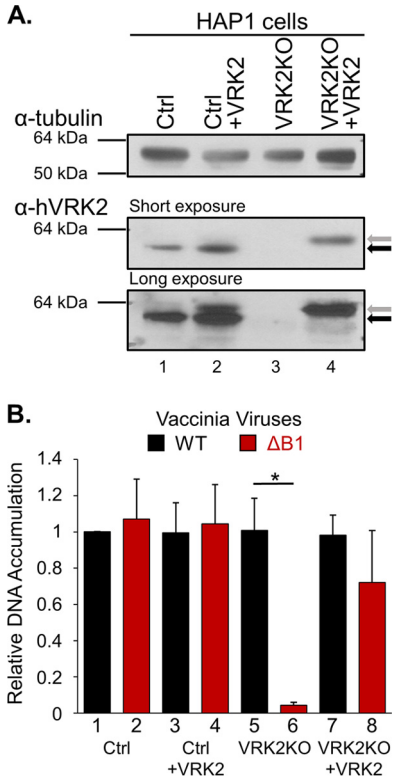

FIG 8 VRK2 reconstitution rescues vvΔB1 deficiency in HAP1 VRK2KO cells. (A) HAP1 control (lanes 1 and 2) and VRK2KO (lanes 3 and 4) cells were transduced with a lentivirus expressing human myc-tagged VRK2 to generate HAP1 control/VRK2myc (lane 2) and VRK2KO/VRK2myc (lane 4) cells. Immunoblot analysis of endogenous VRK2 (black arrow, 58 kDa) and exogenous VRK2myc (gray arrow) was done for each transduced cell line. (B) DNA accumulation was measured after 24-h one-step infection with WT (black) or vvΔB1 (red) virus in control cells (columns 1 and 2), exogenous VRK2myc-expressing control cells (columns 3 and 4), VRK2KO cells (columns 5 and 6), and exogenous VRK2myc-expressing VRK2KO cells (columns 7 and 8). The value for the WT/Ctrl sample was set to 1. Standard deviation is denoted by error bars, and the *P* value is indicated as follows: *, <0.005 (horizontal black lines indicate compared columns).

expression followed a similar trend as observed for the vvΔB1 F18 immunoblot (Fig. 6E); almost all cells express mCherry during vvΔB1 infection of HAP1 control cells, about half do in VRK1KO cells, and very few VRK2KO cells express mCherry protein (Fig. 7, panels 6 to 8). In summary, VRK2 absence and to a lesser extent VRK1 absence resulted in a marked deficiency in vvΔB1 DNA replication, 24-h viral yield, 7-hpi replication factory formation, and 18-hpi late expression of mCherry. These data indicate that endogenous VRK2 can partly compensate for the absence of the B1 kinase during infection of HAP1 cells, specifically during viral DNA replication. Furthermore, endogenous VRK1 was also able to complement the roles of B1 during DNA replication, although to a much lesser degree than VRK2 in these studies.

VRK2 reconstitution in VRK2 knockout HAP1 cells rescues vvΔB1 DNA replication. To confirm the necessity of VRK2 during vvΔB1 infection, we generated a lentivirus expressing the wild-type human *VRK2* gene, tagged at its C terminus with the myc epitope. Stable expression of exogenous VRK2myc was achieved in both HAP1 control cells and VRK2KO HAP1 cells (Fig. 8A). Exogenous VRK2myc (gray arrow) protein levels in the transduced VRK2KO HAP1 cells were similar to protein levels of endogenous VRK2 (black arrow) in HAP1 control cells (Fig. 8A, lanes 1 and 4). Exogenous VRK2myc protein expression in the transduced HAP1 control cells was less than exogenous VRK2myc levels in the VRK2KO HAP1 cells, although they were detectable at a longer exposure (Fig. 8A, lanes 2 and 4). Relative DNA accumulation measurements were used to determine if the addition of exogenous VRK2myc could rescue the

deficiency of the vvΔB1 virus during infection of the VRK2KO HAP1 cell line (Fig. 8B). Exogenous VRK2myc expression in HAP1 control cells did not alter the relative DNA accumulation of the WT or vvΔB1 virus (Fig. 8B, lanes 1 to 4). Importantly, the reconstitution of VRK2 protein in the VRK2KO HAP1 cells resulted in a rescue of the relative DNA accumulation of vvΔB1 16-fold above that in VRK2KO cells (compare columns 6 and 8). These data confirm that the vvΔB1 DNA replication deficiency in the VRK2KO HAP1 cells is due to an absence of VRK2. This is the first demonstration that VRK2 specifically complements for the loss of B1 kinase during viral DNA replication carried out in HAP1 cells.

Impact of VRK2 depletion on vvΔB1 DNA replication in HeLa and A549 cells. Our above-described studies indicate that HAP1 cells are somewhat unique from other cell lines tested (Fig. 5A to D) in that vaccinia virus DNA replication is delayed during vvΔB1 infection but approaches WT levels by 24 hpi (Fig. 6C and D). Therefore, significant reductions in DNA accumulation during vvΔB1 infection of HAP1 cells can be measured effectively, as illustrated in VRK2KO HAP1 cells (Fig. 6C and D). To further examine the requirement of VRK2 during vaccinia virus infection in the absence of B1, we utilized two other human cancer cell lines, HeLa and A549, which express similar protein levels of VRK2 to HAP1 cells (Fig. 9A). First, we used small interfering RNA (siRNA) to deplete VRK2 from either HeLa or A549 cells, using siRNAs targeting VRK2 mRNA. HeLa cells were depleted of VRK2 using two different siRNAs designed to target different sites on the VRK2 mRNA. siVRK2#1 achieved a better depletion than siVRK2#2, resulting in about 20% remaining endogenous VRK2 (Fig. 9B). WT DNA accumulation at 24 hpi was not affected by VRK2 depletion in HeLa cells (Fig. 9C). Notably, vvΔB1 displayed a statistically significant, although modest, decrease in DNA replication during infection of VRK2-depleted HeLa cells in comparison to that during infection of siCtrl HeLa cells. The viral yield of WT virus was not altered, while the vvΔB1 viral yield was modestly reduced during infection of VRK2-depleted HeLa cells (Fig. 9D). Next, endogenous VRK2 was depleted in A549 cells using siVRK2#1. Depletion of VRK2 in A549 cells resulted in $<$20% remaining endogenous VRK2, as assayed using immunoblotting (Fig. 9E). The relative DNA accumulation (Fig. 9F) and viral yield (Fig. 9G) of WT virus were not significantly altered by reduction of endogenous VRK2 from A549 cells. Yet we observed a significant decrease in vvΔB1 DNA accumulation (Fig. 9F) and viral yield (Fig. 9G) in the VRK2-depleted A549 cells. This outcome mirrored the attenuation of vvΔB1 in HAP1 VRK2KO cells (Fig. 6D and F). These data indicate that HAP1 and A549 are cell lines in which vvΔB1 can attain elevated levels of DNA accumulation, enabling us to quantify a significant attenuation during the absence or depletion of VRK2. Moreover, the sufficiency of VRK2 to compensate for B1 during vvΔB1 infection appears to be cell type dependent, as suggested by the differing magnitudes of results in HeLa cells versus HAP1 and A549 cells.

BAF depletion in HAP1 cells lacking VRK2 results in a small increase in vvΔB1 DNA replication. Our next goal was to explore the mechanism through which VRK2 complements for the lack of the B1 viral kinase in vvΔB1. Based on *in vitro* studies confirming the ability of VRK2 to phosphorylate BAF (13), we hypothesized that, like B1, VRK2 may regulate BAF antiviral function in cells; therefore, BAF depletion would rescue vvΔB1 growth in VRK2KO cells. To test this prediction, we transduced HAP1 control and VRK2KO cells to express a BAF-specific shRNA. We then measured viral DNA accumulation during infection with WT virus and vvΔB1 virus in these transduced VRK2KO cells. We found that in cells infected with WT virus, DNA replication was not affected by BAF depletion, consistent with other cell lines (25–27). In comparison, when vvΔB1 DNA accumulation in the VRK2KO shCtrl cells and BAF-depleted cells was measured, a 3.5-fold rescue was observed (Fig. 10A). This increase from 4% to 12% DNA accumulation in comparison to WT infection of VRK2KO shCtrl cells is modest but similar to earlier results for vvΔB1 DNA accumulation in BAF-depleted CV1 cells (Fig. 4C). We therefore posit that VRK2 enhances vvΔB1 DNA replication partially through a BAF-dependent mechanism but also to a significant degree through a BAF-independent mechanism.

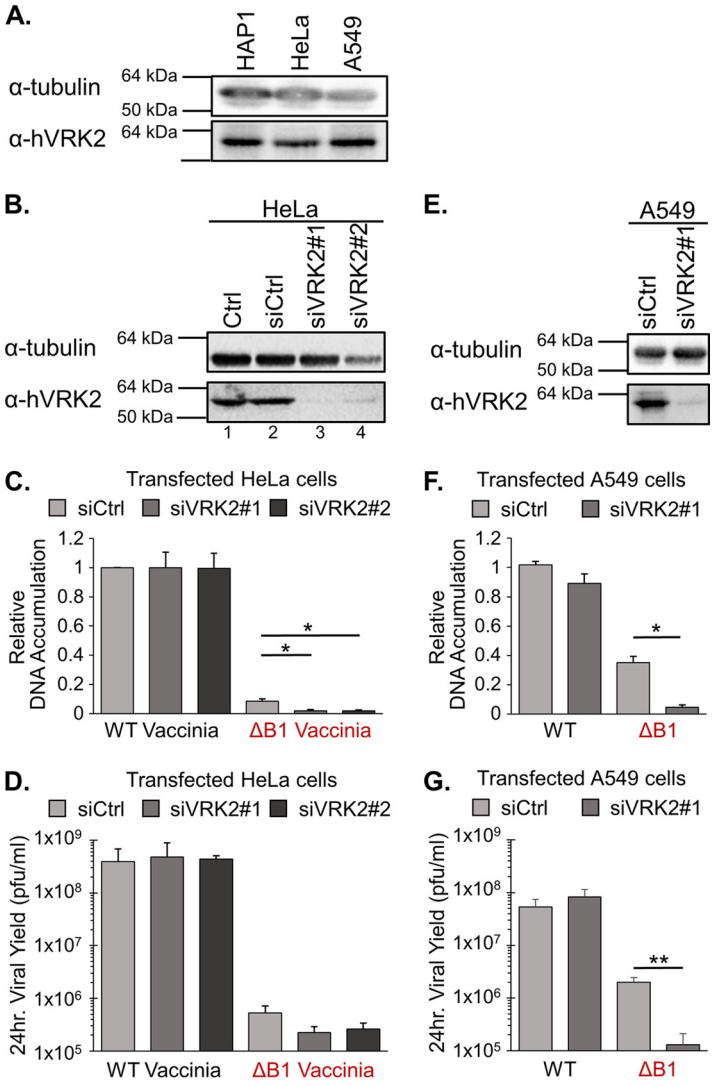

FIG 9 Effect of VRK2 depletion on vvΔB1 growth in human HeLa and A549 cells. (A) Immunoblot analysis of HAP1 control, HeLa, and A549 human cell lysates using anti-tubulin and anti-VRK2 primary antibodies as shown. (B) Endogenous VRK2 was depleted in HeLa cells by transfection of cells with two different siRNAs targeting human VRK2 mRNA. Immunoblot analysis for the tubulin loading control and anti-human VRK2 protein was completed for whole-cell lysates of untransfected HeLa cell control (lane 1), siRNA scrambled as siCtrl (lane 2), and siVRK2#1 (lane 3)- or siVRK2#2 (lane 4)-transfected HeLa cells. (C and D) DNA accumulation (C) and 24-h viral yield (D) assays were completed in siCtrl (light gray bars) and siVRK2#1 (gray bars)- and siVRK2#2 (dark gray bars)-transfected HeLa cells for WT and vvΔB1-infected cells. The value for the WT/HeLa siCtrl sample was set to 1 for DNA accumulation. (E) Endogenous VRK2 was depleted in human A549 cells by transfection of cells with siVRK2#1. Immunoblot analysis of siCtrl and siVRK2#1-transfected A549 cell lysates for detection of the tubulin loading control and human VRK2 protein. (F and G) DNA accumulation (F) and viral yield (G) assays were completed in siCtrl (light gray bars) and siVRK2#1 (gray bars)-transfected CV1 cells for WT (left two columns) and vvΔB1 (right two columns)-infected cells. The value for the WT/A549 siCtrl sample was set to 1 for DNA accumulation. Standard deviation is denoted by error bars, and *P* values are indicated as follows: *, <0.005; **, <0.001 (horizontal black lines indicate compared columns).

To examine whether the loss of VRK2 impacts BAF expression levels or phosphorylation status, we then performed immunoblot analysis of BAF in HAP1 control, VRK1KO, and VRK2KO cells (Fig. 10B). The antibody employed detects both phosphorylated BAF (Fig. 10B, gray arrow), which migrates more slowly in the gel, and the more rapidly migrating unphosphorylated form of BAF (black arrow). In control HAP1 cells, the two forms are detected at similar levels. In VRK1KO cells, there is a clear loss of the upper band representing phosphorylated BAF. These data are consistent with numer-

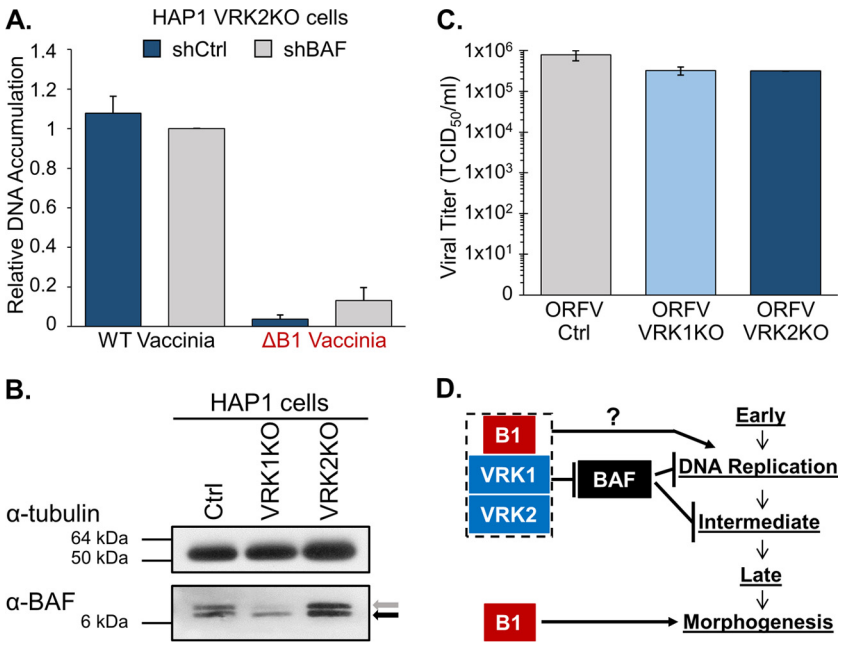

FIG 10 VRK2 rescues vvΔB1 DNA replication primarily through a BAF-independent mechanism. The ORFV life cycle occurs independently of either VRK1 or VRK2 expression from HAP1 cells. (A) DNA accumulation was measured at 24 hpi for WT (left two columns) and vvΔB1 (right two columns) virus in control or BAF-depleted HAP1 VRK2KO cells. The value for the WT/HAP1 VRK2KO shCtrl sample was set to 1. (B) Immunoblot analysis of HAP1 control (lane 1), VRK1KO (lane 2), and VRK2KO (lane 3) cell lysates using anti-tubulin and anti-BAF primary antibodies as shown. (C) HAP1 control, VRK1KO, and VRK2KO cells were infected with the parapoxvirus ORF virus (ORFV) at an MOI of 1 for 4 days. Cells and virus were harvested and titrated on primary ovine fetal turbinate (OFTu) cells and quantified by the Spearman-Karber's 50% tissue culture infectious dose method ($TCID_{50}$/ml). Viral titer values are an average for two replicates, and error bars indicate standard deviations between replicates. (D) Working model of B1- and VRK-regulated vaccinia virus life cycle stages based on this study and previous reports. We identified a B1-VRK2 shared function in BAF regulation and a BAF-independent mechanism, both affecting vaccinia virus DNA replication. B1 was also previously shown to contribute to vaccinia virus morphogenesis.

ous other studies showing that VRK1 plays an important part in modifying the BAF phosphorylation status in the nucleus (13, 16, 17, 35). Interestingly, in VRK2KO cell lysates, there is no apparent loss of the more slowly migrating form of BAF. This lack of a measurable impact of VRK2 on BAF phosphorylation indicates that VRK1 is the dominant BAF kinase in HAP1 cells when measured in whole-cell lysates and leads us to speculate that VRK2-mediated complementation for B1 occurs via a BAF-independent mechanism.

The viral life cycle of ORF virus, naturally lacking the B1 kinase, is not affected by the absence of either cellular VRK1 or VRK2. Our observation that VRK2 can partly complement during infection with vvΔB1 raised the question of whether other viruses lacking a B1 homolog may depend on VRK1 or VRK2 for replication. The ORF virus (ORFV) is a *Poxviridae* family member; however, it is classified under the *Parapoxvirus* genus (1) and lacks a B1-like kinase (36). To explore the role of VRK1 and VRK2 during ORFV infection, we performed a viral growth assay in HAP1 control, VRK1KO, and VRK2KO cells. Interestingly, no significant difference was observed in ORFV viral titers between the control HAP1 cells and either VRK1KO or VRK2KO HAP1 cells (Fig. 10C). These results indicate that neither VRK1 nor VRK2 is required for the viral life cycle of ORFV and that this pathogen has evolved alternative mechanisms to replicate without B1. Consistent with this reasoning, ORFV infection of CV1-B1myc cells did not exhibit enhanced viral fitness compared to control CV1 cells (data not shown). This suggests that ORFV may not rely on cellular VRK1 or VRK2, possibly due to a divergence in evolution from orthopoxviruses. Alternatively, it is plausible that ORFV is capable of utilizing either VRK1 or VRK2 interchangeably in order to replicate its viral DNA. Future

production of a VRK1 VRK2 double knockout cell line will be needed to test this possibility.

DISCUSSION

The sequence identity between the poxvirus B1 protein and the eukaryotic VRKs is striking, approaching 40% within their respective catalytic domains (11). While genes encoding protein kinases are present in other DNA viruses (37), none exhibit this level of sequence identity to any host kinase. Viral mimicry of host signaling components is often an indication of which cellular pathways are manipulated during the course of infection. Thus, our working hypothesis is that B1 and VRKs share substrates important to poxviral replication. This avenue of study has been fruitful in the past, leading to the identification of BAF as a target of both VRKs and B1 (13) and revealing a novel function for BAF in antiviral defense (25). In this article, we characterize a B1-expressing cell line and B1 deletion virus which provide new insights into the function and regulation of this critical viral protein. We then explore the impact of B1 deletion on viral DNA replication in various cell types, focusing our efforts on the question of whether the cellular VRK proteins can complement for the loss of B1 when they are expressed at endogenous levels by the cell.

Previous biochemical and genetic studies of the vaccinia virus B1 kinase utilizing temperature-sensitive viruses uncovered a pivotal role for this protein during genome replication (6). Furthermore, earlier efforts to delete the *B1* gene using homologous recombination were unsuccessful (12), indicating that the fitness cost of B1 deletion is severe. In this study, we have revisited the goal of constructing a B1 knockout virus, relying on a complementing cell line for B1 expression during the isolation of the new virus. The stable expression of B1 in these cells also presented us with an opportunity to characterize B1 in the absence of other viral proteins. We did not observe any difference in growth rate or morphology of cells stably expressing B1, suggesting that expression of this viral kinase is not toxic to CV1 cells. We also found that B1 was present throughout the cytoplasm in uninfected cells, consistent with the fact that it does not possess a sequence predicted to direct localization to the nucleus or other organelles. Interestingly, in infected cells, B1 colocalizes with I3, the viral single-stranded DNA (ssDNA) binding protein and well-established marker of viral replication factories. This recapitulates previous evidence that B1 is present at viral factories (38); however, as B1 is expressed by the cell in our assay, these new data suggest that B1 is actively recruited to sites of vaccinia virus DNA replication. If this is indeed the case, we speculate that recruitment is driven by the ability of B1 to interact with another protein, such as the viral H5 protein rather than viral DNA; B1 has been previously demonstrated to interact with H5 in multiple assays (39, 40), but B1 does not have any domains predicted to directly bind to DNA. Recruitment of B1 to viral factories may enhance its ability to phosphorylate important target proteins, such as the fraction of cellular BAF that is nearest to viral DNA and thus the most imminent threat to the virus. Importantly, however, we found that BAF phosphorylation increases in B1-expressing cells in a manner independent of infection. This extends previous *in vitro* data indicating that other viral proteins are not needed for B1 phosphorylation of BAF (13), but it remains possible that phosphorylation of other B1 substrates depends more heavily on B1 localization to factories.

Our characterization of the B1 deletion virus included direct comparison with the Cts2 virus in multiple assays. As with Cts2, in CV1 cells, the vvΔB1 virus exhibits a marked loss in viral progeny and impairment of viral DNA replication, although in both regards the phenotype of the vvΔB1 virus was more severe than that of Cts2. A significant advantage of studying the vvΔB1 virus is that the phenotype is also robust at 37°C, allowing us to examine B1 function in cell types that cannot tolerate higher temperatures needed for the Cts2 phenotype. Depletion of BAF rescued replication of both Cts2 and the vvΔB1 viruses, reaffirming the B1-BAF signaling axis, although the increase observed during the vvΔB1 infection was notably reduced in comparison to that during Cts2 infection. This observation either demonstrates that BAF remains a

potent antiviral even after depletion or suggests that other important B1 signaling pathways are being disrupted in the complete absence of this kinase.

Positing that the vvΔB1 virus may exhibit some host tropism, due to either cell type-specific complementing kinases or downstream targets, we next examined the ability of this mutant virus to carry out DNA replication and produce new virus in a variety of cell lines. As a result of these studies, it was clear that B1 is vital for the production of new infectious virus in all cell types. However, in regard to DNA accumulation, the cell lines could be grouped into two categories. In BSC40, CV1, L929, and HeLa cells, there was a severe decrease in DNA replication; even when assayed late in infection, the viral DNA from a vvΔB1 infection was 10% or less of that from the WT virus. In contrast, in HAP1 and A549 cells, gross DNA accumulation was slower than WT DNA accumulation but was significant and by 24 h approached WT levels.

We next hypothesized that cellular VRK activity may allow for genome replication in HAP1 and A549 cell lines. To test this theory, we acquired HAP1 cell lines altered at either the *VRK1* or *VRK2* gene using CRISPR (clustered regularly interspaced short palindromic repeat)/Cas9-mediated gene editing. Immunoblot analysis using antibodies specific for each VRK failed to detect VRK1 or VRK2 in the cell line in which that gene had been edited, thus validating these as single knockouts for either VRK1 or VRK2. We also monitored the rate of cell growth for both the knockout and control cells and found that they were very similar. This was a surprising observation, as previous studies have demonstrated that depletion of VRK1 can severely impair growth of MCF10a and MDA-MB-231 cells while also causing mitotic defects linked to reduced BAF phosphorylation (17). Indeed, immunoblot analyses of BAF levels present in VRK1KO cells reveal a clear reduction in the more slowly migrating phosphorylated form of BAF in comparison to the control HAP1 cells, consistent with a decrease in BAF phosphorylation in these cells. Future investigation will be needed to determine why HAP1 cells tolerate the loss of VRK1 during mitosis. Possible mechanisms include the activity of VRK2 or other kinases in the cell, which may substitute for VRK1 in these cells.

Using these HAP1 cell lines, we next compared relative DNA accumulation, protein expression, and productive viral yields during infection with the WT and vvΔB1 viruses. These studies indicated that the loss of VRK1 in HAP1 cells has no effect on the WT virus and only a minimal impact during vvΔB1 infection. In comparison, loss of VRK2 had no significant effect during WT infection but had a striking effect on the vvΔB1 life cycle. Specifically, while early gene expression in vvΔB1-infected cells was unchanged, no DNA accumulation or late gene expression was observed in VRK2KO cells. This robust block in DNA replication culminates in an additional 10-fold inhibition of virus production in comparison to that of the vvΔB1-infected HAP1 control cells. Importantly, VRK2 depletion in A549 cells also decreases vvΔB1 DNA replication and viral yield while having no impact on WT infection, which supports the model that VRK2 functionally overlaps with B1 in these cell lines.

The seminal observation made by Boyle and Traktman (12) that VRK1 can rescue Cts2 replication if expressed from the viral genome laid the groundwork for the discovery of BAF phosphorylation, which is now understood to be a regulator of that protein's antiviral defense and mitotic function. Interestingly, here we show that loss of VRK2 does not result in a discernible change in BAF phosphorylation in HAP1 cells and that BAF depletion has only a very modest effect on DNA replication in vvΔB1-infected VRK2KO cells. Together, these data are consistent with the working model depicted in Fig. 10D. We suggest that VRK2 complements for the loss of B1 via a novel mechanism, likely involving phosphorylation of an important substrate other than BAF. While previous studies from our laboratory indicate that B1 is needed for a step late in the viral life cycle in U2OS cells (8), the data presented here provide a clear indication that B1 is needed at the stage of DNA replication not only to inactivate BAF but also for other reasons in some cells. Furthermore, the functions of B1 cannot be rescued completely by VRKs during the vaccinia virus life cycle (Fig. 10D).

As in the case of the B1-BAF axis where parallel study of VRK1 was insightful, future study of VRK2 and B1 will likely yield clues regarding which other pathways are

modulated by the B1 kinase. Published research on VRK2 provides a list of candidate signaling cascades which may be involved. For example, VRK2 has been reported to modulate MAP kinase signaling pathways at the ER, in part via an interaction with the KSR scaffolding protein (41, 42). Additionally, VRK2 appears to act as an apoptosis regulator in some studies, inhibiting cell death via interaction with Bcl-xL or by altering BAX gene expression (18). An investigation of these pathways in conjunction with structure/function studies of VRK2 are ongoing in our laboratory. Those studies will shed light on the molecular mechanism underlying VRK2 and B1 function, providing greater insight into how host and viral signaling converge during poxviral infection.

MATERIALS AND METHODS

Chemicals and primers. Unless otherwise noted, chemicals were obtained from Sigma-Aldrich. Primers were obtained from Integrated DNA Technologies.

Cell culture. African green monkey kidney CV1 cells were obtained from Invitrogen Life Technologies. African green monkey BSC40, mouse fibroblast L929, human cervix epithelial adenocarcinoma HeLa, and human lung epithelial carcinoma A549 cells were purchased and obtained directly from the ATCC. These cell lines except A549 cells were maintained in Dulbecco's modified Eagle's medium (DMEM) supplemented with 10% fetal bovine serum (FBS; Atlanta Biologicals) and penicillin-streptomycin in 5% CO_2 at 37°C. A549 cells were maintained in DMEM/Ham's F-12 nutrient mixture (1:1) medium supplemented with 10% FBS and penicillin-streptomycin under conditions stated above. Human near-haploid fibroblast HAP1 parental, vaccinia virus-related kinase 1 (VRK1) knockout (VRK1KO), and VRK2KO cells were obtained from Horizon Genomics and maintained in Iscove's modified Dulbecco's medium (IMDM; Fisher Scientific) with 10% FBS and penicillin-streptomycin under incubation conditions as stated above. VRK1KO cells (catalog no. HZGHC000073c014) contain an 11-bp deletion in VRK1 exon 5 introduced by CRISPR/Cas9 gene editing, and VRK2KO cells (catalog no. HZGHC000403c006) contain a 7-bp deletion in VRK2 exon 2.

Primary ovine fetal turbinate (OFTu) cells were obtained by aseptically removing turbinate tissues from ovine fetuses and minced in the presence of phosphate-buffered saline (PBS) and antibiotics, washed several times with PBS, digested with 0.2% trypsin at room temperature (RT) for 1 to 2 h, and gauze filtered. The cell suspension was centrifuged, and pellets were washed twice with PBS and once with growth medium. Cells were maintained in minimal essential medium (MEM) supplemented with 10% FBS, 2 mM L-glutamine, and 50 μg/ml of gentamicin.

Viruses and viral infection assays. The following viruses were used: wild-type vaccinia virus (WR strain), B1-deficient Cts2 virus (4), B1 deletion vaccinia virus, and ORF virus (ORFV) (36). The B1 deletion recombinant vaccinia virus vvΔB1 was generated by infecting B1myc-expressing CV1 cells with WT virus (MOI = 0.03) and cotransfecting the linear DNA fragment upB1-P11-mCherry-downB1 (Integrated DNA Technologies). This DNA fragment was synthesized to contain the mCherry ORF under the control of the vaccinia P11 promoter (43) and flanked by sequence homologous to the 250 bp immediately upstream and downstream of the B1 ORF; thus, it was constructed to replace the B1 ORF with P11mCherry upon homologous recombination. The infected/transfected cells were incubated for 48 h, harvested, and titrated on B1-expressing CV1 cells for isolation of individual plaques. Virus expressing mCherry was purified by serial plaque purification on CV1-B1myc cells until no nonfluorescent plaques (out of 100 plaques) were observed. The vvΔB1 virus was plaque purified six additional times before being expanded on B1myc-expressing CV1 cells and purified using a sucrose cushion. Replacement of the B1 ORF was verified by DNA sequencing and PCR analysis (primer sequences available upon request). Parapoxvirus ORFV (OV-IA82 strain) was isolated, propagated, and purified in OFTu cells. Genomic DNA sequencing confirmed homogenous virus stock preparation. ORFV passaged fewer than 10 times after plaque purification was used for experiments (Fig. 10C).

For plaque assays, CV1 cells transduced with the indicated vectors were infected with WT, Cts2, or vvΔB1 virus at 200 PFU per well at 39.7°C and fixed/stained 48 hpi. For immunofluorescence assays, cell lines were infected with WT or vvΔB1 virus at an MOI of 5 at 37°C for 7 or 18 h prior to fixation with 4% paraformaldehyde (PFA). For viral DNA replication assays, cells infected with WT, Cts2, or vvΔB1 virus (MOI = 3) were incubated at 37°C or 39.7°C (only for studies including Cts2) and harvested at the times postinfection indicated in the figure legend, pelleted, and resuspended in PBS before DNA purification using a GeneJET whole-blood genomic DNA purification minikit K0782 from Thermo Scientific. The viral DNA was quantified as detailed in the quantitative PCR (qPCR) protocol below (see "DNA purification and qPCR"). For vaccinia viral yield analysis, cells were infected with WT, Cts2, or vvΔB1 virus at an MOI of 3, incubated at 37°C or 39.7°C (only for studies including Cts2), harvested at 24 hpi, and resuspended in 10 mM Tris (pH 9). Virus samples were freeze-thawed three times and titrated on B1myc-expressing CV1 cells at 37°C or 31.5°C (only for experiments including Cts2) for plaque assays. For immunoblotting analysis shown in Fig. 3A, CV1 cells were infected with WT or vvΔB1 virus at an MOI of 10 at 37°C, and cells were harvested 6 hpi. For the immunoblotting analysis shown in Fig. 6E, HAP1 cell lines were infected with WT or vvΔB1 virus at an MOI of 3 at 37°C, and cells were harvested 7 and 18 hpi for early and late protein detection, respectively.

ORFV viral yield was assayed for ORFV infection (MOI = 1) of HAP1 control, VRK1KO, and VRK2KO cells. Four days postinfection, cells were harvested and lysed. Cell debris was pelleted using centrifugation, and supernatants containing virus were used to quantitate viral yield by the Spearman-Karber's 50%

tissue culture infectious dose method ($TCID_{50}$/ml), using primary ovine fetal turbinate (OFTu) cells. A viral yield experiment (Fig. 10C) was performed in experimental duplicates.

Generation of stably transduced cell lines. The pHAGE-HYG-MCS-B1myc construct was produced by amplifying a codon-optimized myc-tagged B1 ORF using the BamHI-Kozak-B1 (5′-AGCAGGATCCGC CACCATGAACTTC-3′) forward primer and the B1-BamHI (5′-GGCGGATCCTTACAGGTCCTCTTCAG-3′) reverse primer and cloning the product into the BamHI site of the multiple cloning site of the pHAGE-HYG-MCS vector (17).

Lentiviruses encapsidating pHAGE-HYG-B1myc were produced in 293T cells following transfection with pHAGE-HYG-MCS-B1myc or pHAGE-HYG-MCS (empty vector) in combination with pVSVG, pTat, pREV, and pGag/Pol. At 15.5 h posttransfection, fresh medium with 5 mM sodium butyrate was added to the cells. At 24 h posttransfection, fresh medium with 10 mM HEPES (Fisher Scientific) was added to the cells. At 48 h posttransfection, recombinant virus was harvested, Polybrene (Fisher Scientific) was added at 10 μg/ml, and stocks were aliquoted for storage at −80°C. These lentiviruses were used to transduce CV1 cells the day following cell seeding at 3×10^5 cells in a 35-mm well. B1myc and control CV1 cells were selected with 200 μg/ml hygromycin (Invitrogen), and B1myc expression was confirmed by immunoblotting using mouse anti-myc (Myc-Tag [9B11] mouse monoclonal antibody 2276; Cell Signaling) antibody or plaque assay rescue of vvΔB1 virus on B1myc-expressing CV1 cells.

Lentiviruses expressing BAF-specific short hairpin RNA (shRNA) or control (scrambled) shRNA have been described previously (25) and were used for stable depletion of BAF in CV1 cells and HAP1 VRK2KO cells. Those transduced cells were selected with 10 μg/ml and 500 ng/ml of puromycin, respectively, prior to use in experiments. Lentiviral vector pLenti-C-Myc-DDK expressing myc-tagged human VRK2 (isoform VRK2A, RC206522L1; OriGene) was used to generate lentivirus as described above.

siRNA depletion. Small interfering RNAs (siRNAs) targeting human VRK2 and nontargeting scrambled siRNAs were designed and ordered from Dharmacon. Two different siRNAs targeting all isoforms of human VRK2 were designed. The siRNA sense sequences used were as follows: VRK2#1, 5′-CACAAUAG GUUAAUCGAAAUU-3′; VRK2#2, 5′-ACGUUCAGAUCCUCUAUU-3′; nontargeting scrambled control (siCtrl), 5′-CAGUCGCGUUUGCGACUGGUU-3′. HeLa or A549 cells were transfected with 100 nM siRNA using Lipofectamine RNAiMAX (Life Technologies) in accordance with the manufacturer's suggestions. Protein depletion was measured by immunoblot analysis at 3 days posttransfection. For one-step infections in siRNA-treated cells, cells were split into a 12-well plate 3 days posttransfection and infected 4 days posttransfection prior to 24-h DNA accumulation and viral yield assays.

Immunofluorescence analysis. Cells were fixed with 4% paraformaldehyde (Alfa Aesar) and treated with 0.2% Triton X-100 (Sigma) for 10 min at RT to permeabilize cellular membranes. Following washes, the mouse anti-myc (1:100, 9B11 Cell Signaling) and rabbit anti-I3 (1:300, custom antibody [44]) primary antibodies were incubated 1 h at RT and used to detect myc-tagged B1 and I3 early protein, respectively. Washes were followed by incubation with Fluor 488-conjugated goat anti-mouse and Fluor 594-conjugated goat anti-rabbit (1:400, Life Technologies) secondary antibodies for 2 h at RT (Fig. 1C [myc only] and 2B). Alternatively, Fluor 488-conjugated goat anti-rabbit secondary antibody (1:400; Life Technologies) was incubated for 2 h at RT (Fig. 7). All cells were incubated with 4′,6-diamidino-2-phenylindole (DAPI) nuclear stain. All dilutions and washes used 1× Dulbecco's phosphate-buffered saline (DPBS)/modified with Ca^+ and Mg^+ added (HyClone Thermo Scientific). Immunofluorescence images were taken using a EVOS FL auto cell imaging system (Invitrogen) with dual cameras and the selected green fluorescent protein (GFP; Fluor 488), Texas Red (Fluor 594 and mCherry), and DAPI excitation/emission filters. Composites were generated to correct brightness and LUT settings, and images were saved as RGB.tiff or montage.tiff files using ImageJ software.

Immunoblotting analysis. To evaluate protein expression, control or B1myc-expressing CV1 cells (1×10^6) were harvested and resuspended to 1×10^5 cells/μl in SDS sample buffer supplemented with 10 U/ml of benzonase or Pierce universal nuclease for cell lysis (Thermo Scientific), trypsin serine protease inhibitor (phenylmethylsulfonyl fluoride), protease inhibitor cocktail (Roche), and phosphatase inhibitor cocktail (Roche). Lysate volumes equivalent to 3×10^5 cells for detection of B1myc protein or 1×10^5 cells for detection of total BAF or phosphorylated BAF and tubulin control were resolved on a 12% SDS-PAGE gel for B1myc or an 18% SDS-PAGE gel for BAF and tubulin detection. Protein was transferred overnight onto a polyvinylidene difluoride (PVDF) membrane, and the membrane was blocked in 5% milk. Mouse anti-myc (1:1,000, 9B11; Cell Signaling), rabbit anti-BAF (1:3,000, custom antibody [28]), rabbit anti-phospho-BAF (1:1,000, custom antibody [28]), and mouse anti-tubulin (1:10,000, T7816; Sigma-Aldrich) primary antibodies for B1myc, total BAF, phosphorylated BAF, and tubulin were used, respectively, with appropriate horseradish peroxidase-conjugated goat anti-mouse or goat anti-rabbit (1:20,000; Bio-Rad) secondary antibodies, followed by incubation with Supersignal WestPico chemiluminescent reagents (Thermo Scientific). Quantification of chemiluminescence signals were performed using Bio-Rad ImageLab software, and images were obtained using film and developer.

To determine protein expression in HAP1 control, VRK1KO, or VRK2KO cells, cells were harvested and prepared as detailed above for lysate volumes equivalent to 1×10^5 cells/μl. Lysates for VRK1 and VRK2 blots were resolved on a 12% SDS-PAGE gel, and lysates for BAF, tubulin, I3, and F18 blots were resolved on an 18% SDS-PAGE gel. Proteins were transferred onto a PVDF membrane, followed by blocking with 5% milk. Mouse anti-humanVRK1 (1:500, E-3; sc-390809; Santa Cruz Biotechnology), mouse anti-humanVRK2 (1:500, H-5; sc-365199; Santa Cruz Biotechnology), rabbit anti-BAF, mouse anti-tubulin, rabbit anti-I3 (1:2,000, custom antibody), and rabbit anti-F18 (1:6,000, custom antibody) primary antibodies were used to detect VRK1, VRK2, total BAF, tubulin, I3 vaccinia early protein, and F18 vaccinia late protein, respectively. Secondary antibody incubation followed the protocol detailed above. All blots except VRK1 and VRK2 blots were incubated with chemiluminescent reagent as detailed above. Both

VRK1 and VRK2 blots were incubated with Supersignal WestFemto maximum sensitivity substrate chemiluminescent reagents (Thermo Scientific). Quantitation and imaging of blots used the same protocols as detailed above.

DNA purification and qPCR. Viral DNA was extracted from infected cells (the infection protocol is detailed in "Viruses and viral infection assays") and purified using a GeneJET whole-blood genomic DNA purification minikit (K0782; Thermo Scientific). Quantitative PCR was performed using Bio-Rad iTaq Universal SYBRGreen supermix by following a protocol detailed previously (28). In brief, serial dilutions were completed for each experiment, and qPCR was run to develop a standard curve and determine amplification efficiency. About 10 ng DNA and 1 μM primers in a single well reaction were completed in technical triplicates for each sample. DNA quantification used primers F (5′-CATCATCTGGAATTGTCA CTACTAAA-3′) and R (5′-ACGGCCGACAATTATAATTAATGC-3′), which are specific for the vaccinia virus HA gene.

Statistics. Each experimental question was tested in a minimum of three experimental replicates, unless stated otherwise, and graphed data represent the mean of all experimental replicates. Error bars shown represent standard deviations from the mean. The *P* values indicated were calculated using two-tailed Student's *t* tests.

ACKNOWLEDGMENTS

This research was supported through NIH grants to M.S.W. (R01AI114653) and the Nebraska Center for Virology (P30GM10359), which supported certain aspects of these studies such as the Morrison Microscopy Core Facility at UNL. A.T.O. was supported partly through a training grant (T32AI125207).

The contents of the manuscript are solely the responsibility of the authors and do not necessarily represent the official views of the NIH.

A.T.O. and M.S.W. conceived the idea and designed the experiments along with A.B.R., Z.W., and G.D.; A.T.O. made vaccinia viral stocks and performed immunofluorescence assays; A.T.O., A.B.R., and Z.W. performed Western blot analyses, viral yield studies, and siRNA studies; G.D. performed experiments using the ORF virus; A.T.O. and M.S.W. wrote the manuscript, with critiques provided by all other authors.

REFERENCES

1. Moss B. 2013. Poxviridae, p 2129. *In* Knipe DM, Howley PM (ed), Fields virology, 6th ed, vol 2. Lippincott Williams and Wilkins, Philadelphia, PA.
2. Yang Z, Cao S, Martens CA, Porcella SF, Xie Z, Ma M, Shen B, Moss B. 2015. Deciphering poxvirus gene expression by RNA sequencing and ribosome profiling. J Virol 89:6874–6886. https://doi.org/10.1128/JVI.00528-15.
3. Bratke KA, McLysaght A, Rothenburg S. 2013. A survey of host range genes in poxvirus genomes. Infect Genet Evol 14:406–425. https://doi.org/10.1016/j.meegid.2012.12.002.
4. Condit RC, Motyczka A, Spizz G. 1983. Isolation, characterization, and physical mapping of temperature-sensitive mutants of vaccinia virus. Virology 128:429–243. https://doi.org/10.1016/0042-6822(83)90268-4.
5. Rempel RE, Anderson MK, Evans E, Traktman P. 1990. Temperature-sensitive vaccinia virus mutants identify a gene with an essential role in viral replication. J Virol 64:574–583.
6. Rempel RE, Traktman P. 1992. Vaccinia virus B1 kinase: phenotypic analysis of temperature-sensitive mutants and enzymatic characterization of recombinant proteins. J Virol 66:4413–4426.
7. Kovacs GR, Vasilakis N, Moss B. 2001. Regulation of viral intermediate gene expression by the vaccinia virus B1 protein kinase. J Virol 75:4048–4055. https://doi.org/10.1128/JVI.75.9.4048-4055.2001.
8. Jamin A, Ibrahim N, Wicklund A, Weskamp K, Wiebe MS. 2015. Vaccinia B1 kinase is required for post-replicative stages of the viral lifecycle in a BAF-independent manner in U2OS cells. J Virol 89:10247–10259. https://doi.org/10.1128/JVI.01252-15.
9. Nezu J, Oku A, Jones MH, Shimane M. 1997. Identification of two novel human putative serine/threonine kinases, VRK1 and VRK2, with structural similarity to vaccinia virus B1R kinase. Genomics 45:327–331. https://doi.org/10.1006/geno.1997.4938.
10. Zelko I, Kobayashi R, Honkakoski P, Negishi M. 1998. Molecular cloning and characterization of a novel nuclear protein kinase in mice. Arch Biochem Biophys 352:31–36. https://doi.org/10.1006/abbi.1998.0582.
11. Nichols RJ, Traktman P. 2004. Characterization of three paralogous members of the mammalian vaccinia related kinase family. J Biol Chem 279:7934–7946. https://doi.org/10.1074/jbc.M310813200.
12. Boyle KA, Traktman P. 2004. Members of a novel family of mammalian protein kinases complement the DNA-negative phenotype of a vaccinia virus ts mutant defective in the B1 kinase. J Virol 78:1992–2005. https://doi.org/10.1128/JVI.78.4.1992-2005.2004.
13. Nichols RJ, Wiebe MS, Traktman P. 2006. The vaccinia-related kinases phosphorylate the N′ terminus of BAF, regulating its interaction with DNA and its retention in the nucleus. Mol Biol Cell 17:2451–2464. https://doi.org/10.1091/mbc.E05-12-1179.
14. Blanco S, Klimcakova L, Vega FM, Lazo PA. 2006. The subcellular localization of vaccinia-related kinase-2 (VRK2) isoforms determines their different effect on p53 stability in tumour cell lines. FEBS J 273:2487–2504. https://doi.org/10.1111/j.1742-4658.2006.05256.x.
15. Kang T, Park D, Choi YH, Kim K, Yoon HS, Kim K. 2007. Mitotic histone H3 phosphorylation by vaccinia-related kinase 1 in mammalian cells. Mol Cell Biol 27:8533–8546. https://doi.org/10.1128/MCB.00018-07.
16. Gorjanacz M, Klerkx EP, Galy V, Santarella R, Lopez-Iglesias C, Askjaer P, Mattaj IW. 2007. Caenorhabditis elegans BAF-1 and its kinase VRK-1 participate directly in post-mitotic nuclear envelope assembly. EMBO J 26:132–143. https://doi.org/10.1038/sj.emboj.7601470.
17. Molitor TP, Traktman P. 2014. Depletion of the protein kinase VRK1 disrupts nuclear envelope morphology and leads to BAF retention on mitotic chromosomes. Mol Biol Cell 25:891–903. https://doi.org/10.1091/mbc.E13-10-0603.
18. Monsalve DM, Merced T, Fernandez IF, Blanco S, Vazquez-Cedeira M, Lazo PA. 2013. Human VRK2 modulates apoptosis by interaction with Bcl-xL and regulation of BAX gene expression. Cell Death Dis 4:e513. https://doi.org/10.1038/cddis.2013.40.
19. Li LY, Liu MY, Shih HM, Tsai CH, Chen JY. 2006. Human cellular protein VRK2 interacts specifically with Epstein-Barr virus BHRF1, a homologue of Bcl-2, and enhances cell survival. J Gen Virol 87:2869–2878. https://doi.org/10.1099/vir.0.81953-0.
20. Teferi WM, Dodd K, Maranchuk R, Favis N, Evans DH. 2013. A whole-genome RNA interference screen for human cell factors affecting myxoma virus replication. J Virol 87:4623–4641. https://doi.org/10.1128/JVI.02617-12.
21. Zheng R, Ghirlando R, Lee MS, Mizuuchi K, Krause M, Craigie R. 2000. Barrier-to-autointegration factor (BAF) bridges DNA in a discrete, higher-

order nucleoprotein complex. Proc Natl Acad Sci U S A 97:8997–9002. https://doi.org/10.1073/pnas.150240197.
22. Furukawa K, Sugiyama S, Osouda S, Goto H, Inagaki M, Horigome T, Omata S, McConnell M, Fisher PA, Nishida Y. 2003. Barrier-to-autointegration factor plays crucial roles in cell cycle progression and nuclear organization in Drosophila. J Cell Sci 116:3811–3823. https://doi.org/10.1242/jcs.00682.
23. Puente XS, Quesada V, Osorio FG, Cabanillas R, Cadinanos J, Fraile JM, Ordonez GR, Puente DA, Gutierrez-Fernandez A, Fanjul-Fernandez M, Levy N, Freije JM, Lopez-Otin C. 2011. Exome sequencing and functional analysis identifies BANF1 mutation as the cause of a hereditary progeroid syndrome. Am J Hum Genet 88:650–656. https://doi.org/10.1016/j.ajhg.2011.04.010.
24. Paquet N, Box JK, Ashton NW, Suraweera A, Croft LV, Urquhart AJ, Bolderson E, Zhang SD, O'Byrne KJ, Richard DJ. 2014. Nestor-Guillermo progeria syndrome: a biochemical insight into barrier-to-autointegration factor 1, alanine 12 threonine mutation. BMC Mol Biol 15:27. https://doi.org/10.1186/s12867-014-0027-z.
25. Wiebe MS, Traktman P. 2007. Poxviral B1 kinase overcomes barrier to autointegration factor, a host defense against virus replication. Cell Host Microbe 1:187–197. https://doi.org/10.1016/j.chom.2007.03.007.
26. Ibrahim N, Wicklund A, Wiebe MS. 2011. Molecular characterization of the host defense activity of the barrier to autointegration factor against vaccinia virus. J Virol 85:11588–11600. https://doi.org/10.1128/JVI.00641-11.
27. Ibrahim N, Wicklund A, Jamin A, Wiebe MS. 2013. Barrier to autointegration factor (BAF) inhibits vaccinia virus intermediate transcription in the absence of the viral B1 kinase. Virology 444:363–373. https://doi.org/10.1016/j.virol.2013.07.002.
28. Jamin A, Wicklund A, Wiebe MS. 2014. Cell- and virus-mediated regulation of the barrier-to-autointegration factor's phosphorylation state controls its DNA binding, dimerization, subcellular localization, and antipoxviral activity. J Virol 88:5342–5355. https://doi.org/10.1128/JVI.00427-14.
29. Skoko D, Li M, Huang Y, Mizuuchi M, Cai M, Bradley CM, Pease PJ, Xiao B, Marko JF, Craigie R, Mizuuchi K. 2009. Barrier-to-autointegration factor (BAF) condenses DNA by looping. Proc Natl Acad Sci U S A 106:16610–16615. https://doi.org/10.1073/pnas.0909077106.
30. Molitor TP, Traktman P. 2013. Molecular genetic analysis of VRK1 in mammary epithelial cells: depletion slows proliferation in vitro and tumor growth and metastasis in vivo. Oncogenesis 2:e48. https://doi.org/10.1038/oncsis.2013.11.
31. López-Sánchez I, Sanz-García M, Lazo PA. 2009. Plk3 interacts with and specifically phosphorylates VRK1 in Ser342, a downstream target in a pathway that induces Golgi fragmentation. Mol Cell Biol 29:1189–1201. https://doi.org/10.1128/MCB.01341-08.
32. Vinograd-Byk H, Sapir T, Cantarero L, Lazo PA, Zeligson S, Lev D, Lerman-Sagie T, Renbaum P, Reiner O, Levy-Lahad E. 2015. The spinal muscular atrophy with pontocerebellar hypoplasia gene VRK1 regulates neuronal migration through an amyloid-β precursor protein-dependent mechanism. J Neurosci 35:936–942. https://doi.org/10.1523/JNEUROSCI.1998-14.2015.
33. Kang TH, Park DY, Kim W, Kim KT. 2008. VRK1 phosphorylates CREB and mediates CCND1 expression. J Cell Sci 121:3035–3041. https://doi.org/10.1242/jcs.026757.
34. Valbuena A, López-Sánchez I, Lazo PA. 2008. Human VRK1 is an early response gene and its loss causes a block in cell cycle progression. PLoS One 3:e1642. https://doi.org/10.1371/journal.pone.0001642.
35. Lancaster OM, Cullen CF, Ohkura H. 2007. NHK-1 phosphorylates BAF to allow karyosome formation in the Drosophila oocyte nucleus. J Cell Biol 179:817–824. https://doi.org/10.1083/jcb.200706067.
36. Delhon G, Tulman ER, Afonso CL, Lu Z, de la Concha-Bermejillo A, Lehmkuhl HD, Piccone ME, Kutish GF, Rock DL. 2004. Genomes of the parapoxviruses ORF virus and bovine papular stomatitis virus. J Virol 78:168–177. https://doi.org/10.1128/JVI.78.1.168-177.2004.
37. Jacob T, Van den Broeke C, Favoreel HW. 2011. Viral serine/threonine protein kinases. J Virol 85:1158–1173. https://doi.org/10.1128/JVI.01369-10.
38. Banham AH, Smith GL. 1992. Vaccinia virus gene B1R encodes a 34-kDa serine/threonine protein kinase that localizes in cytoplasmic factories and is packaged into virions. Virology 191:803–812. https://doi.org/10.1016/0042-6822(92)90256-O.
39. McCraith S, Holtzman T, Moss B, Fields S. 2000. Genome-wide analysis of vaccinia virus protein-protein interactions. Proc Natl Acad Sci U S A 97:4879–4884. https://doi.org/10.1073/pnas.080078197.
40. Beaud G, Beaud R, Leader DP. 1995. Vaccinia virus gene H5R encodes a protein that is phosphorylated by the multisubstrate vaccinia virus B1R protein kinase. J Virol 69:1819–1826.
41. Blanco S, Santos C, Lazo PA. 2007. Vaccinia-related kinase 2 modulates the stress response to hypoxia mediated by TAK1. Mol Cell Biol 27:7273–7283. https://doi.org/10.1128/MCB.00025-07.
42. Fernandez IF, Perez-Rivas LG, Blanco S, Castillo-Dominguez AA, Lozano J, Lazo PA. 2012. VRK2 anchors KSR1-MEK1 to endoplasmic reticulum forming a macromolecular complex that compartmentalizes MAPK signaling. Cell Mol Life Sci 69:3881–3893. https://doi.org/10.1007/s00018-012-1056-8.
43. Esposito J, Brechling K, Baer G, Moss B. 1987. Vaccinia virus recombinants expressing rabiesvirus glycoprotein protect against rabies. Virus Genes 1:7–21.
44. Rochester SC, Traktman P. 1998. Characterization of the single-stranded DNA binding protein encoded by the vaccinia virus I3 gene. J Virol 72:2917–2926.
45. Cullen CF, Brittle AL, Ito T, Ohkura H. 2005. The conserved kinase NHK-1 is essential for mitotic progression and unifying acentrosomal meiotic spindles in Drosophila melanogaster. J Cell Biol 171:593–602. https://doi.org/10.1083/jcb.200508127.
46. Condit RC, MA. 1981. Isolation and preliminary characterization of temperature-sensitive mutants of vaccinia virus. Virology 113:224–241. https://doi.org/10.1016/0042-6822(81)90150-1.